Reanalysis of the ^{7}Be$(p,\gamma)^8$B S factor in a microscopic model

P. Descouvemont
Physique Nucléaire Théorique et Physique Mathématique, CP229 Université Libre de Bruxelles, B1050 Brussels, Belgium
(Received 15 September 2004; published 6 December 2004)

A previous microscopic three-cluster calculation, applied to the ^{7}Be$(p,\gamma)^8$B reaction, is updated in several ways: the ^{7}Be description is improved, two nucleon-nucleon interactions are considered, and new experimental information about the scattering lengths is taken into account. Weak changes in the energy dependence of the S factor are obtained. A "theoretical" uncertainty is estimated. It amounts to 5% near 1 MeV but reaches more than 10% when energy increases. We suggest that reducing the current uncertainty on the experimental scattering length would significantly reduce the error bar on $S_{17}(0)$. Elastic ^{7}Be$+p$ phase shifts are briefly discussed and analyzed for different ^{7}Be deformations. We show that the differences with the potential model are due to shortcomings of that model, such as the lack of ^{7}Be deformation, included in the present approach. We also investigate the ^{8}Li and ^{8}B spectroscopy, electromagnetic transition probabilities, and spectroscopic factors. The ^{5}He$+^3$H configuration (or mirror) is shown to be important in the ground-state structure.

DOI: 10.1103/PhysRevC.70.065802 PACS number(s): 21.60.Gx, 24.10.Cn, 25.40.Lw, 27.20.+n

I. INTRODUCTION

The ^{7}Be$(p,\gamma)^8$B S factor is one of the main inputs in the solar neutrino problem, as ^{8}B decay provides high-energy neutrinos which can be detected in terrestrial experiments [1]. Recent experiments were able to determine the neutrino flux emitted from ^{8}B decay with a precision of 9% [1]. On the other hand, theoretical predictions are more uncertain, of the order of 20% [2–4]. The theoretical neutrino flux sensitively depends on the ^{7}Be$(p,\gamma)^8$B S factor (hereafter denoted as S_{17}) which should be known with a high precision [5].

Many experimental and theoretical groups have been working on S_{17} in recent years (see, e.g., Ref. [6] for a review). Experimentally, two types of methods are used: direct methods [6–10] where a proton beam is used on a ^{7}Be target and indirect methods [11,12] using a ^{8}B beam, which subsequently breaks up into ^{7}Be and p. Both methods present advantages and limitations, which we do not discuss here. Their common problem is the need for theoretical models to derive S_{17} at stellar energies. As is well known [13], nuclear astrophysics involves very low energies where, in general, cross sections between charged particles are too small to be measured in the laboratory. In the ^{7}Be$(p,\gamma)^8$B reaction, the Gamow energy is about 20 keV whereas the current lower limit in direct experiments is about 100 keV.

Theoretical calculations of S_{17} have been performed with several methods: the R-matrix parametrization [14], the potential model [15–17], and microscopic cluster models [18–20]. In parallel, the asymptotic normalization constant (ANC) method may help in determining $S_{17}(0)$ (see Ref. [21] for a recent review). As the ^{8}B ground state is weakly bound with respect to the ^{7}Be$+p$ threshold (-137 keV), the capture process is essentially external and the cross section at low energies is determined from the asymptotic properties of the ^{8}B wave function which depends on a single parameter, the ANC [22].

In recent experimental works, the data are extrapolated down to zero energy by using a microscopic three-cluster model (Ref. [18], referred to as DB94). In this model the only inputs are a nucleon-nucleon (NN) interaction, chosen in DB94 as the Volkov force [23], and a cluster structure for ^{8}B. The deformation of ^{7}Be is taken into account by using an $\alpha+^3$He cluster wave function. Microscopic models are based on basic principles of quantum mechanics, such as the Pauli principle between nucleons, and therefore present a rather strong predictive power. Of course their precision is limited by uncertainties on the nucleon-nucleon interaction (choice of the nucleon-nucleon force, three-body terms, etc.). For poorly known reactions microscopic models provide valuable information, such as the presence of resonances or estimates of the cross sections. The situation is different for S_{17} where a very high precision is required. In this context it is clear that the normalization provided by a microscopic model should be considered as an upper limit only [24]. Consequently, analyses of recent experiments are done by using the energy dependence of DB94, leaving the normalization as a free parameter.

The motivation of the present work is to update the results of DB94 by using the same model with improved conditions of calculation. Preliminary results were presented in Ref. [25] but are superseded by the present ones. Reconsidering S_{17} in a microscopic model is justified by several reasons.

(i) In DB94, the ^{7}Be nucleus is deformed, but its structure is "frozen" and it cannot be distorted during the collision. In 1994, this was a necessary assumption to keep computer times in reasonable limits, but this approximation is not required anymore with current computers.

(ii) Only Volkov forces were considered in DB94. In the present work we also used the Minnesota interaction [26] which is known to be better adapted to low-mass systems. The slightly different results obtained with both forces contribute to the model uncertainty.

(iii) In DB94, uncertainties due to the model itself are not analyzed. This forces experimental groups either to neglect model uncertainties or to fix a somewhat arbitrary uncertainty on the theoretical S_{17}. The sensitivity to the model is addressed here.

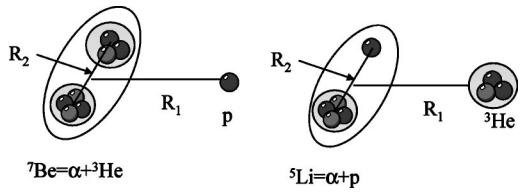

FIG. 1. Three-cluster configurations of ^{8}B.

(iv) A recent measurement of the ^{7}Be$+p$ elastic cross section [27] provides the scattering lengths. These data can be used as a constraint on the model.

(v) A recent calculation by Davids and Typel [17], performed within the potential model, provides an energy dependence significantly different from DB94. At first sight, this simple model seems to be more consistent than DB94 with breakup data [12], and the differences need to be understood.

The paper is organized as follows. In Sec. II we briefly present the model, which is essentially the same as in DB94. Section III is devoted to spectroscopic properties of ^{8}Li and ^{8}B. These results are used to test the model and to evaluate its precision. The ^{7}Li$(n,\gamma)^8$Li and ^{7}Be$(p,\gamma)^8$B cross sections are analyzed in Sec. IV. Concluding remarks are given in Sec. V.

II. MICROSCOPIC THREE-CLUSTER MODEL

Here we present a brief overview of the model. More detail can be found in Refs. [28,29]. As in DB94, we assume that the eight nucleons of the system are divided in three clusters, with two arrangements channels: ^{7}Be$+p$ and ^{5}Li $+^3$He. A total wave function is therefore given by

$$\Psi^{JM\pi} = \Psi^{JM\pi}_{7+1} + \Psi^{JM\pi}_{5+3}, \tag{1}$$

where J is the total spin and π the total parity. In the resonating group method (RGM) each component is written as [30]

$$\Psi^{JM\pi}_{a+b} = \sum_{\gamma} \mathcal{A}[Y_L(\Omega_{\rho_1}) \otimes [\phi^{I_a}_a \otimes \phi^{I_b}_b]^S]^{JM} g^{J\pi}_{\gamma}(\rho_1), \tag{2}$$

where ρ_1 is the relative distance, $\mathcal{A}$ the antisymmetrization operator, and $(\phi^{I_a}_a, \phi^{I_b}_b)$ are microscopic wave functions of nuclei a and b; in Eq. (2), L is the relative angular momentum, S is the channel spin, and γ stands for $\gamma=(I_a, I_b, S, L)$.

In two-cluster studies, the internal wave functions $\phi^{I_a}_a$ and $\phi^{I_b}_b$ are defined in the shell model. This approximation is, however, not well adapted to the ^{7}Be$+p$ system, as ^{7}Be presents a significant deformation. Consequently, ^{7}Be is described by an $\alpha+^3$He cluster structure and its wave function is defined by

$$\phi^{I_a M_a}_7 = \mathcal{A}\phi^0_4[Y_\ell(\Omega_{\rho_2}) \otimes \phi^{1/2}_3]^{I_a M_a} g^{I_a}_{7,\ell}(\rho_2), \tag{3}$$

where ρ_2 is the relative distance between α and ^{3}He (see Fig. 1), ℓ is the relative angular momentum, and ϕ^0_4 and $\phi^{1/2}_3$ are shell-model wave functions of α and ^{3}He, respectively. A similar expression holds for the ^{5}Li nucleus.

In practical applications, the relative wave functions are expanded over a Gaussian basis, which corresponds to the generator coordinate method (GCM—see Ref. [31]). For ^{7}Be, we have

$$g^{I_a}_{7,\ell}(\rho_2) = \int f^{I_a}_{7,\ell}(R_2)\Gamma_\ell(\rho_2, R_2) dR_2 \approx \sum_{n=1}^{N_2} f^{I_a}_{7,\ell}(R_{2n})\Gamma_\ell(\rho_2, R_{2n}), \tag{4}$$

where R_2 is the generator coordinate associated with the $\alpha+^3$He system and $\Gamma_\ell(\rho,R)$ is a projected Gaussian function (see, for example, Ref. [32]). As is well known, the Gaussian expansion (4), when inserted in to Eq. (3), provides the wave function as a linear combination of projected Slater determinants. In the GCM, the calculation of the relative function $g(\rho_2)$ is replaced by the calculation of the generator function $f(R_2)$.

In order to analyze the ^{7}Be wave functions, let us consider Fig. 2, where we present the binding energy of ^{7}Be for different R_2 values. The calculation is done with the Volkov V2 and Minnesota (referred to as MN) interactions (more detail is given in Sec. III). Figure 2 clearly confirms the importance of clustering effects. The minimum of the ground-state energy curve ($I_a=3/2^-$) is obtained near 3.5 fm. In DB94, where only the V2 force was considered, a single value for R_2 was used ($R_2=3.7$ fm). In the present case, in order to allow distortion effects during the collision, five generator coordinates are included (1.1–6.3 fm in steps of 1.3 fm). The mixing of these basis functions provides the ^{7}Be spectrum in the right panel of Fig. 2 which shows, for both *NN* interactions, a fairly good agreement with experiment.

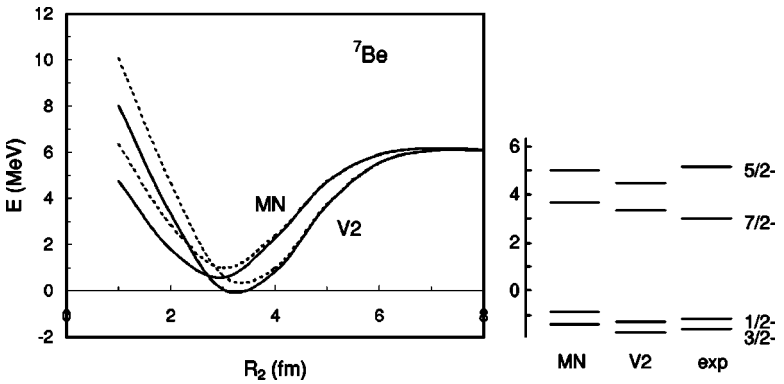

FIG. 2. Left panel: energy of ^{7}Be as a function of the generator coordinate R_2, for $I_a=3/2^-$ (solid lines) and $I_a=1/2^-$ (dotted lines). Right panel: energy spectra with the MN and V2 interactions.

Let us now consider the eight-nucleon wave functions (2). The relative function $g_\gamma^{J\pi}(\rho_1)$ is expanded over a Gaussian basis with generator coordinate R_1 (see Fig. 1). As shown in Ref. [28], this allows us to rewrite the wave function (2) as

$$\Psi_{a+b}^{JM\pi} = \sum_\gamma \int F_\gamma^{J\pi}(R_1,R_2)\Phi_\gamma^{JM\pi}(R_1,R_2)dR_1dR_2, \qquad (5)$$

where $\Phi_\gamma^{JM\pi}(R_1,R_2)$ is an eight-nucleon projected Slater determinant and $F_\gamma^{J\pi}(R_1,R_2)$ is the three-cluster generator function. As before, the integrals over the generator coordinates are replaced by finite sums.

Owing to the Gaussian expansion, the wave functions (5) do not have a correct asymptotic behavior. This is solved by using the microscopic R-matrix method (MRM; see Ref. [32]) which restores the Coulomb behavior of scattering states as well as of bound states. Basically, the generator function in Eq. (5) is determined from matrix elements of the Hamiltonian between projected Slater determinants $\Phi_\gamma^{JM\pi}(R_1,R_2)$. The double angular momentum projection (on $\alpha+^3$He and ^{7}Be$+p$) yields five-dimensional integrals [28], but can be easily performed with modern computers.

III. SPECTROSCOPIC PROPERTIES OF ^{8}Li AND ^{8}B

A. Conditions of the calculation

As mentioned previously, we use here the Volkov V2 [23] and Minnesota interactions [26], complemented by a zero-range spin-orbit force [33]. The amplitude S_0 of the spin-orbit interaction is taken as $S_0=20$ MeV fm^5 for MN and $S_0=26$ MeV fm^5 for V2. These values provide a good excitation energy of the $1/2^-$ state in ^{7}Be. The parameters u and M of the MN and V2 forces are adjusted on the ^{8}B ground-state energy. As we will consider different conditions of calculation, these parameters will vary slightly. For the full calculation, we have $u=1.0736$ and $M=0.5744$ for ^{8}B. These values are reasonably close to the standard values ($u=1$ and $M=0.6$).

The internal wave functions are defined with an oscillator parameter $b=1.43$ fm which represents a compromise between the optimal values of α and ^{3}He. The ^{7}Be wave functions include five generator coordinates R_2 ranging from 1.1 fm to 6.3 fm (with step 1.3 fm). For ^{5}Li, we have four values (1.1–5.0 fm with a step of 1.3 fm). As in DB94, the $3/2^-$, $1/2^-$, $7/2^-$, and $5/2^-$ partial waves of ^{7}Be are included (the lowest states are shown in Fig. 2); for ^{5}Li, we take account of the $3/2^-$ and $1/2^-$ dominant partial waves. The relative motion associated with ^{7}Be$+p$ (and ^{5}Li$+^3$He) is described by ten generator coordinates, ranging from 2.0 fm to 10.1 fm with a step of 0.9 fm.

B. ^{8}Li and ^{8}B nuclei

In addition to the capture cross sections, the same model can be applied to the spectroscopy of ^{8}Li and ^{8}B. The properties of ^{8}Li are given in Table I and compared with experiment. In general the difference between the MN and V2 forces is weak. As expected [24], the V2 interaction gives stronger clustering effects, which results in larger quadrupole moments and $E2$ transition probabilities. The values obtained here are similar to those of DB94, where less accurate wave functions were used. In general the agreement with experiment is acceptable, except for the $B(E2,1^+\to 2^+)$ whose experimental value [34,35] is unexpectedly large [36].

TABLE I. Spectroscopic properties of ^{8}Li.

	MN	V2	Expt.[a]
$Q(2^+)$ (e fm^2)	2.3	2.5	2.4±0.2,[b] 3.27±0.06
$\mu(2^+)$ (μ_N)	1.20	1.26	1.65
$\Gamma_n(3^+)$ (keV)	37	43	33±6
$B(M1,1^+\to 2^+)$ (W.u.)[c]	4.1	3.8	2.8±0.9
$B(M1,3^+\to 2^+)$ (W.u.)	0.09	0.15	0.29±0.13
$B(E2,1^+\to 2^+)$ (W.u.)	1.2	2.3	47±23,[d] 87±23[e]
$B(E2,3^+\to 2^+)$ (W.u.)	4.3	5.9	

[a]Reference [37].
[b]Reference [38].
[c]W.u.=Weisskopf units.
[d]Reference [34].
[e]Reference [35].

The same quantities are given in Table II for the ^{8}B nucleus. Comments similar to those of ^{8}Li can be done. The agreement with experiment is reasonable and the sensitivity with respect to the NN interaction is weak. As in DB94, the magnetic moment is found larger in ^{8}B than in ^{8}Li. This is in contradiction with experiment and suggests that the NN interaction might need a tensor component to account for the magnetic moments.

C. Spectroscopic factors and ANC's

The present calculation offers the possibility to analyze the ^{8}B and ^{8}Li wave functions and, more precisely, their spectroscopic factors and ANC's. The ANC in a channel γ is obtained from the asymptotic part of the relative function [39]. Using the notation of Eq. (2), we have

$$g_\gamma^{J\pi}(\rho) \to C_\gamma^{J\pi} W_{-\eta_\gamma L+1/2}(2\kappa_\gamma\rho), \qquad (6)$$

where η_γ and κ_γ are the Sommerfeld parameter and wave number in channel γ and $C_\gamma^{J\pi}$ is the ANC. Here index γ is complemented by a further index labeling the $7+1$ and 5

TABLE II. Spectroscopic properties of ^{8}B.

	MN	V2	Expt.[a]
$Q(2^+)$ (e fm^2)	6.0	6.6	6.83±0.21
$\mu(2^+)$ (μ_N)	1.52	1.48	1.03
$\Gamma_p(1^+)$ (keV)	57	56	37±5
$\Gamma_p(3^+)$ (keV)	390	450	350±40
$B(M1,1^+\to 2^+)$ (W.u.)	3.8	3.4	5.1±2.5
$B(M1,3^+\to 2^+)$ (W.u.)	0.09	0.11	
$B(E2,1^+\to 2^+)$ (W.u.)	4.3	9.7	
$B(E2,3^+\to 2^+)$ (W.u.)	3.5	5.0	

[a]Reference [37].

TABLE III. Amplitudes N_γ, spectroscopic factors S_γ, and ANC's C_γ (in fm$^{-1/2}$) of ^{8}B and ^{8}Li.

	^{8}B(2^+)			^{8}Li(2^+)			^{8}Li(1^+)		^{8}Li(3^+)	
Channel γ	N_γ	S_γ	C_γ	N_γ	S_γ	C_γ	N_γ	S_γ	N_γ	S_γ
^{7}Be$(1/2^-)+p$, $S=0$							0.056	0.129	0.001	0.002
^{7}Be$(1/2^-)+p$, $S=1$	0.091	0.211	0.382	0.092	0.226	0.446	0.208	0.499	0.002	0.004
^{7}Be$(3/2^-)+p$, $S=1$	0.089	0.194	0.334	0.093	0.216	0.332	0.240	0.537	0.000	0.001
^{7}Be$(3/2^-)+p$, $S=2$	0.386	0.836	−0.746	0.361	0.835	−0.798	0.041	0.087	0.273	0.462
^{5}Li$(1/2^-)+^3$He, $S=0$							0.011	0.030	0.014	0.039
^{5}Li$(1/2^-)+^3$He, $S=1$	0.033	0.089	−11.040	0.030	0.083	−7.000	0.033	0.086	0.012	0.034
^{5}Li$(3/2^-)+^3$He, $S=1$	0.037	0.096	−6.783	0.038	0.101	−4.410	0.341	0.840	0.099	0.271
^{5}Li$(3/2^-)+^3$He, $S=2$	0.304	0.815	19.880	0.318	0.871	13.420	0.032	0.087	0.244	0.673

+3 rearrangement channels. The ANC's of the ^{8}B ground state are given in Table III for the MN potential. As found previously [40], the $S=2$ channel dominates. The ANC's of ^{8}B and ^{8}Li are very similar, as expected from simple theoretical arguments and confirmed by experiment (see Ref. [41]). Experimental data [21,42] are obtained in another coupling mode, where the nucleon angular momentum is first coupled to the nucleon spin and the resulting spin j is coupled to the spin 3/2 of the core. The ANC's in this coupling mode are related to the present values by $C^2_{p3/2}=(C_{S=1}-C_{S=2})^2/2$ and $C^2_{p1/2}=(C_{S=1}+C_{S=2})^2/2$. From Table III we have $C^2_{p3/2}=0.583$ fm^{-1} for ^{8}B and $C^2_{p3/2}=0.638$ fm^{-1} for ^{8}Li. These values are larger than the experimental ANC's derived from distorted-wave Born approximation (DWBA) analyses (0.388 ± 0.039 fm^{-1} [42] and 0.384 ± 0.038 fm^{-1} [21], respectively). The ratios $C^2_{p1/2}/C^2_{p3/2}$ (0.146 and 0.170) are closer to experiment (0.157 and 0.125 for ^{8}B and ^{8}Li, respectively). The ^{7}Be(p, γ)^{8}B reaction being essentially external [43], $S_{17}(0)$ can be estimated from the ANC's only [44]. Using the values of Table III provides $S_{17}(0)\approx 25$ eV b.

The relative wave functions $g^{J\pi}_\gamma(\rho)$ appearing in Eq. (2) cannot be directly interpreted without the antisymmetrization operator [45], as they are known to be affected by the Pauli-forbidden states. Their effects cancel out with the antisymmetrizor but provide spurious terms without this operator. More physical wave functions can be defined by applying the overlap kernel on the relative functions $g^{J\pi}_\gamma(\rho)$. Two definitions are useful:

$$\tilde{g}^{J\pi}_\gamma(\rho)=\sum_{\gamma'}\int \mathcal{N}^{J\pi}_{\gamma,\gamma'}(\rho,\rho')g^{J\pi}_{\gamma'}(\rho')d\rho',$$

$$\hat{g}^{J\pi}_\gamma(\rho)=\sum_{\gamma'}\int [\mathcal{N}^{J\pi}_{\gamma,\gamma'}(\rho,\rho')]^{1/2}g^{J\pi}_{\gamma'}(\rho')d\rho', \qquad (7)$$

where $\mathcal{N}^{J\pi}_{\gamma\gamma'}(\rho,\rho')$ is the overlap kernel (see Refs. [45,46] for more detail). Notice that the overlap kernel acts at small distances only and that the three relative functions present the same asymptotic behavior. They are computed numerically using the method presented in Ref. [47].

From Eqs. (7), one defines the amplitude

$$N^{J\pi}_\gamma=\int_0^\infty [\hat{g}^{J\pi}_\gamma(\rho)]^2d\rho \qquad (8)$$

and the spectroscopic factor

$$\mathcal{S}^{J\pi}_\gamma=\int_0^\infty [\tilde{g}^{J\pi}_\gamma(\rho)]^2d\rho. \qquad (9)$$

By definition $\hat{g}^{J\pi}_\gamma(\rho)$ is normalized to unity and we have

$$\sum_\gamma N^{J\pi}_\gamma=1. \qquad (10)$$

This is different for the spectroscopic factor which is not normalized to unity. Those numbers provide an estimate of the weights of the different channels. In the wave functions $\hat{g}^{J\pi}_\gamma(\rho)$, the antisymmetrization is treated approximately. Accordingly, the values of $N^{J\pi}_\gamma$, although rigorously defined mathematically, should not be considered as precise weights of the different channels [because of antisymmetrization, components associated with different channels in the wave function (2) are not orthogonal to each other].

The amplitudes and spectroscopic factors are also given in Table III. In all states, the 5+3 channels are not negligible. This is not surprising in bound states or narrow resonances since, at short distances, the antisymmetrization makes the 7+1 and 5+3 configurations almost equivalent. For the 2^+ state, the main component is $S=2$, whereas for the 1^+ state, $S=1$ dominates. The ^{7}Be $(1/2^-)+p$ component of the ^{8}B ground state is 9.1%, in good agreement with a recent experimental measurement of Cortina-Gil *et al.* [48], who find (13 ± 3)%. The structure of the 3^+ state is more exotic. The main component comes from the ^{7}Be$(5/2^-)+p$ channel ($N=0.35$), as it corresponds to an angular momentum $L=1$. As for the 2^+ and 1^+ states, the 5+3 channels are non-negligible.

In Table IV, we compare the ^{8}Li spectroscopic factors with the experimental data [49,50]. The data are obtained from ^{7}Li$(d,p)^8$Li stripping measurements, which provide the spectroscopic factors through a DWBA analysis. The values are therefore partly model dependent and should not be considered as very precise. The theoretical values are obtained by summing the individual contributions of the channels spins $S=1$ and $S=2$. In general we overestimate the data,

TABLE IV. ^{8}Li spectroscopic factors.

State	GCM	Expt. [49]	Expt. [50]
2^+	1.05	0.88	0.87
1^+	0.62	0.47	0.48
3^+	0.47	0.25	

which is consistent with the overestimation of the neutron widths (see Table I). For the ground state, our result is very close to an R-matrix analysis of Barker [14], who fits ^{7}Li$(n,\gamma)^8$Li data and finds $\mathcal{S}(2^+)=1.034$.

IV. CAPTURE CROSS SECTIONS

A. ^{7}Li$(n,\gamma)^8$Li cross section

The calculation of the capture cross sections requires wave functions for scattering states. As scattering lengths a_S for the ^{7}Li+n and ^{7}Be+p systems are available [27,51], we have determined the interaction parameters u (for MN) or M (for V2) on the a_2 values, relative to the channel spin $S=2$ [(-3.63 ± 0.05) fm for ^{7}Li+n and (-7 ± 3) fm for ^{7}Be+p]. In the full calculation, for example, we have $u=1.07$ and $M=0.563$ for ^{7}Be+p. The scattering length is not expected to significantly affect the low-energy S_{17} [27]. However, it may have some influence on the energy dependence of the S factor.

First, we analyze the ^{7}Li$(n,\gamma)^8$Li mirror reaction. Figure 3 displays the cross section in two different energy ranges.

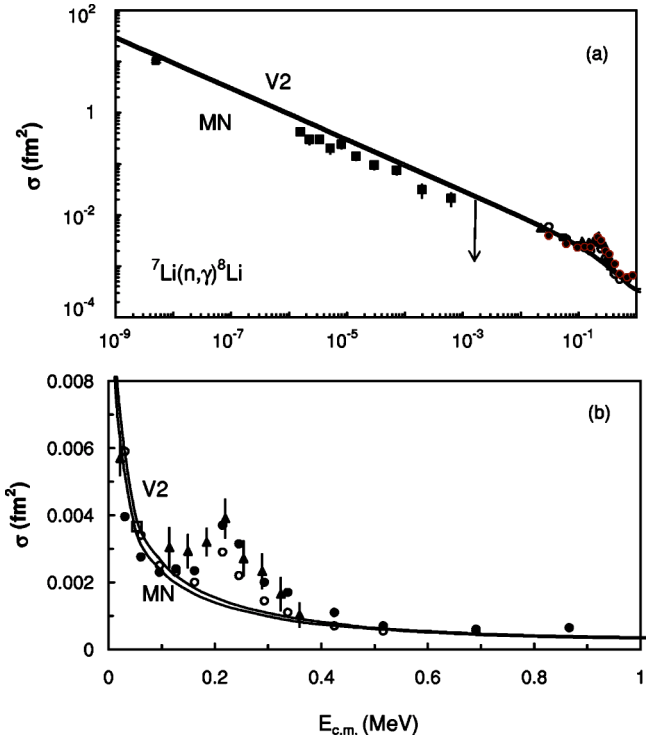

FIG. 3. ^{7}Li$(n,\gamma)^8$Li cross section. Experimental data are taken from Refs. [52] (triangles), [53] (open squares), [54] (solid squares), and [55] (circles).

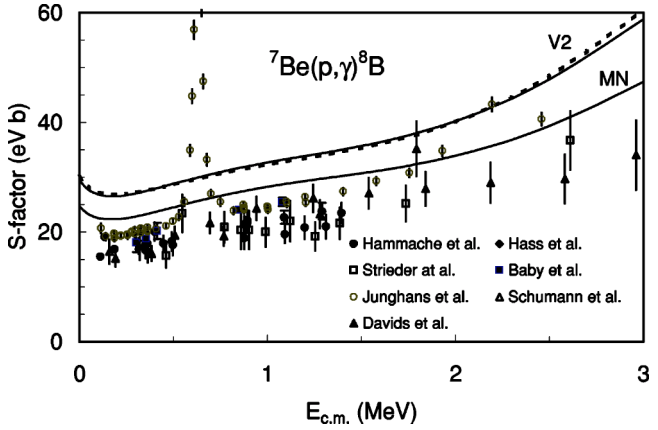

FIG. 4. ^{7}Be$(p,\gamma)^8$B S factor for the V2 and MN interactions. Experimental data are taken from Refs. [6–12]. The results of DB94 are shown as a dashed line.

The data of Wiescher *et al.* [52] have been renormalized as suggested by Heil *et al.* [53]. The cross section is given by the contribution of the 2^+ ground state and of the 1^+ first excited state. The branching ratio is about 10%, in agreement with experiment. At low energies, the cross section behaves as $1/v$ (v is the relative velocity), as expected for s-wave capture. Both NN interactions, however, slightly overestimate the data of Blackmon *et al.* [54]. Above 0.01 MeV, the calculation is consistent with the data of Wiescher *et al.* [52]. The present cross section is quite similar to the results of DB94 (notice that the $M1$ contribution, involving the 3^+ resonance near 0.2 MeV, is not included here).

B. ^{7}Be$(p,\gamma)^8$B cross section

The S_{17} curves are given in Fig. 4 (numerical values are given in the Appendix). According to Ref. [56] we do not use the direct data of Refs. [57–59] and the indirect data of Refs. [60,61] as not enough information is provided about the analysis and normalization procedure. Notice that the breakup data of the GSI group [12] are under reanalysis and are expected to be in better agreement with direct experiments [62]. Figure 4 shows that improving the GCM basis does not significantly change S_{17}. The present V2 results are very close to DB94, obtained with the same interaction. However, as expected from the ANC's (see Table III), the S_{17} values obtained with the MN force are lower and closer to experiment. This was already observed in Ref. [19]. As discussed in DB94, a cluster model provides an upper bound of the capture cross section. The "exact" ^{8}B wave function should contain many other configurations (other arrangements, four clusters, etc.). Accordingly, the capture cross section, which, up to the electromagnetic operator, is nothing but the overlap between the initial ^{7}Be+p and final ^{8}B wave functions, is in general overestimated by a cluster model.

In Fig. 5, we provide the different contributions to S_{17}. As the MN force is known to be better adapted to low-mass systems and as it does provide a better normalization, we only consider the MN potential. Both for s and d waves, the $S=2$ component is larger than $S=1$. This is consistent with the spectroscopic factors of Table III. At zero energy the L

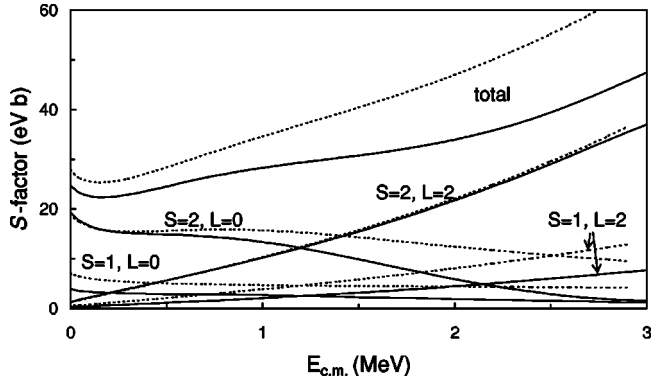

FIG. 5. (S,L) components of S_{17}. Dotted lines correspond to the potential model of Davids and Typel [17].

$=2$ contribution is about 10% of the total S factor. Each component is compared with the potential-model calculation of Davids and Typel [17]. The slope of the S factor above 1 MeV is larger in their model than in the GCM. We will come back to this difference later, but the decomposition of Fig. 5 clearly shows that it arises from the $S=2$, $L=0$ contribution.

Even if the present MN calculation provides a significant improvement regarding the normalization, it is likely that the energy dependence is still more accurate than the normalization itself. Figure 6 shows the energy dependence, normalized to unity at zero energy. Below 200 keV, all curves are almost undistinguishable, as expected from simple arguments. The MN and V2 curves present slight differences with respect to DB94. The strongest difference is obtained with the MN force around 1 MeV ($\pm 10\%$). In order to understand the difference with the potential model [17], we have considered intermediate calculations with a limited basis. We have taken a single value for the ^{7}Be generator coordinate R_2 and the $^7\mathrm{Be}(3/2^-)+p$ configuration only. In each case, the interaction has been readjusted on the ^{8}B ground-state energy and on the $^7\mathrm{Be}+p$ scattering length ($S=2$). Figure 6 clearly shows that, when R_2 tends to zero—i.e., when the conditions of the GCM get closer to the potential-model approximations—both theoretical approaches are similar. The remaining differences are due to antisymmetrization effects and to different interactions. Above 0.5 MeV, the weaker slope in the GCM is due to the ^{7}Be deformation, absent in the potential model. The curve labeled by "mixing" is obtained by considering all R_2 values, but neglecting excited $^7\mathrm{Be}+p$ channels and the $5+3$ configuration. The role of those channels is a further reduction of the S_{17} slope between 1 and 3 MeV.

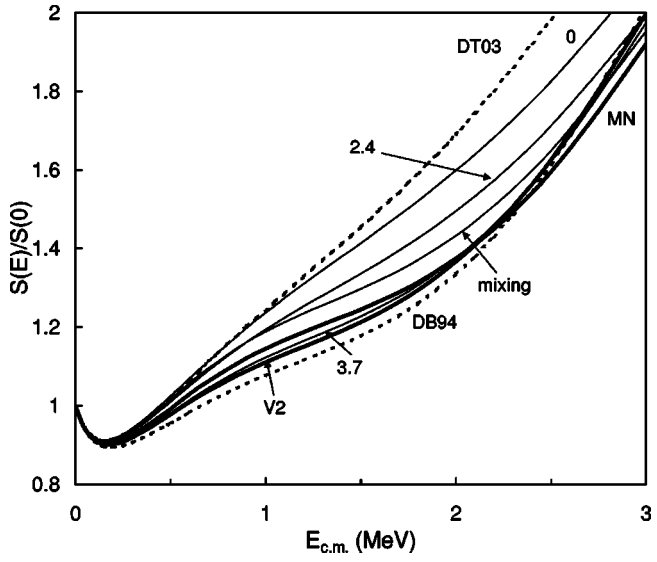

FIG. 6. Energy dependence of S_{17} for different generator coordinates R_2 (thin curves) and for the full calculations (thick curves). The results of DB94 and of the potential model [17] (labeled as DT03) are shown as dashed lines.

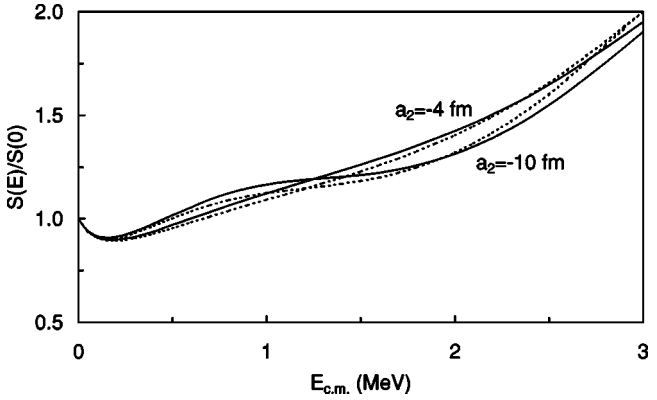

FIG. 7. Influence of the scattering length a_2 on the energy dependence of S_{17} for the MN (solid curves) and V2 (dashed curves) interactions.

C. Theoretical uncertainties in S_{17}

One of the main issues in extrapolating the data down to zero energy is to derive uncertainties in S_{17}. In addition to the usual experimental error bars, a theoretical uncertainty should be included. It is almost impossible to establish a rigorous theoretical uncertainty but some guidelines can be derived. In the present work, we evaluate it from three origins: (i) the NN interaction, (ii) the scattering length, and (iii) the scaling uncertainty, which measures how stable is the energy dependence when the conditions of the calculation are changed.

The uncertainty due to the *NN* interaction is determined from the differences between the V2 and MN forces. Of course, other forces could be considered, but this choice is typical of cluster models. The effect of the scattering length is illustrated in Fig. 7, where a_2 has been changed to -4 and -10 fm—i.e., within the experimental limits. The effect of a variation on a_2 is similar for both interactions. As shown in Ref. [27], the effect of a large and negative a_2 value is equivalent to a broad 2^- resonance near 3 MeV. This led Barker and Mukhamedzhanov [63] to suggest the existence of a 2^- resonance from an R-matrix approach. The width is however so large ($\Gamma \geqslant 4$ MeV) that this broad state should be considered more as a mathematical way to fit the data than as a physical ^{8}B state. The effect of the scattering length in the

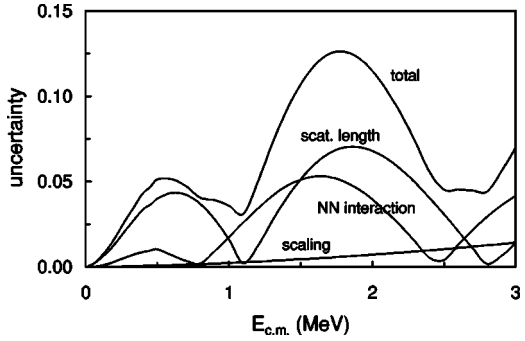

FIG. 8. Contributions to the uncertainties in the energy dependence of the S factor (see text).

energy dependence of S_{17} is lower than 5% below 1 MeV but can reach 10% near 2 MeV.

In order to use theoretical models in the data extrapolation, it is implicitly assumed that the theoretical curve can be rescaled by a factor which does not depend on energy. This is of course a shortcoming since the proportionality is valid at low energies only, where the capture essentially proceeds at large distances. In order to evaluate the validity of the "scaling" approximation, we have used the potential model, with a Woods-Saxon potential as in Ref. [17]. The range has been varied from 2.2 fm to 2.8 fm, and the depth has been changed accordingly. The relative differences in S_{17} are plotted in Fig. 8, which confirms that this effect increases with energy. Of course this scaling effect is just a first estimate as it comes from the potential model. However, it turns out to be lower than uncertainties due to the *NN* interaction and to the scattering lengths.

The three components are given in Fig. 8. Between 0 and 1 MeV the main uncertainty comes from the scattering length (4% at most). Beyond 1 MeV the choice of the *NN* interaction also plays a role. The total uncertainty has been evaluated by summing all contributions. Figure 8 shows that, even at 0.5 MeV, the theoretical uncertainty is still 5% and increases above 1 MeV. The 6% uncertainty due to theory, as evaluated by Davids and Typel [17], is close to our recommendation.

D. ^{7}Be+p phase shifts

The phase shifts characterize the wave functions at large distances. They are plotted in Fig. 9, where we illustrate different conditions of calculation for s waves (see Sec. IV B). For the $S=2$ channel spin, the *NN* interaction is determined to reproduce the experimental scattering length. Hence, all calculations are equivalent up to $E\approx 1$ MeV—i.e., in the energy range where the scattering-length expansion should be valid. As for the ^{7}Be$(p,\gamma)^8$B cross section, the GCM phase shifts get closer to the potential model [17] if we reduce deformation effects in ^{7}Be. The full calculation, including inelastic channels, is significantly different from the potential model.

For $S=1$, the scattering length has not been fitted, as it is experimentally less accurate and as it represents a small contribution to S_{17}. The scattering length is negative for all conditions of calculations. The comparison with the potential model is therefore meaningless, since the scattering lengths have opposite signs.

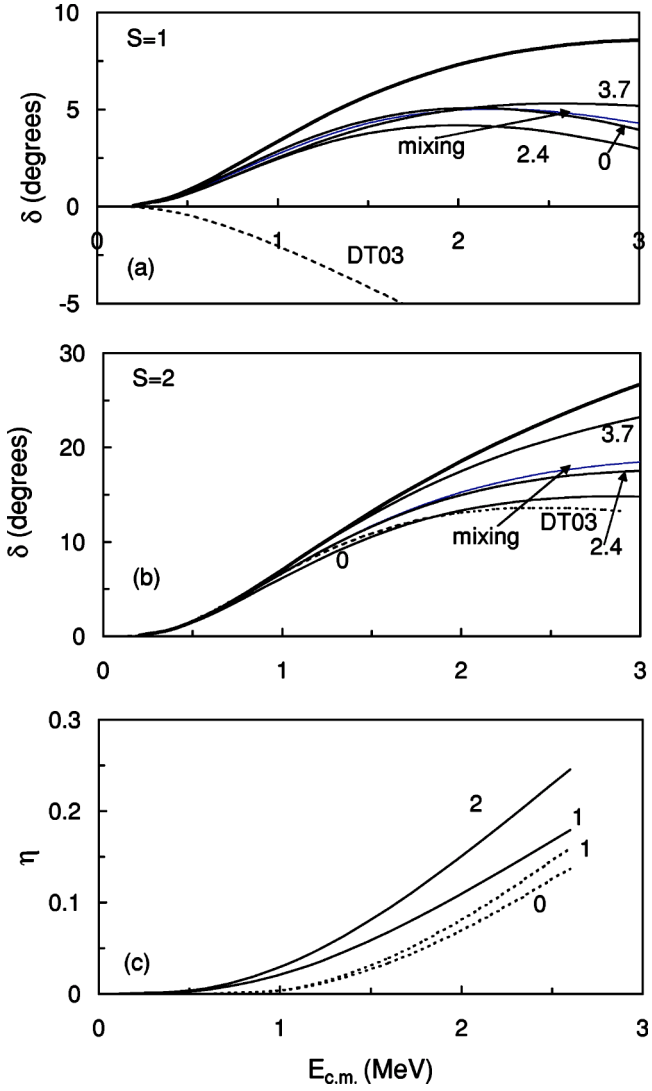

FIG. 9. s-wave ^{7}Be+p phase shifts for $S=1$ (a) and $S=2$ (b) and amplitude η (c). (a) and (b) The curves are labeled by the generator coordinate R_2. The thick curves correspond to the full calculation and the dotted curves to Ref. [17]. (c) Transmission amplitude from the $(J=2^-,L=0)$ channel to the ^{7}Be$(3/2^-)+p$ (solid curves) and ^{7}Be$(1/2^-)+p$ (dotted curves) channels; the labels correspond to the channel spin S (see text).

In Fig. 9(c), we show the amplitude η defined from the collision matrix U as

$$U^{J\pi}_{\gamma,\gamma'} = \eta^{J\pi}_{\gamma,\gamma'} \exp(2i\delta^{J\pi}_{\gamma,\gamma'}). \tag{11}$$

Here, the entrance channel γ is taken as $S=2$, $L=0$ $(J=2^-)$ and the exit channels γ' are $(S=1,L=2)$ and $(S=2,L=2)$ (solid curves). Transfer to the ^{7}Be$(1/2^-)+p$ channel is illustrated with $(S=0,L=2)$ and $(S=1,L=2)$. The amplitude η is a measurement of the coupling between different channels. It is small at astrophysical energies, but turns out to be non-negligible above 1 MeV. In addition to the deformation ef-

fects mentioned previously, this coupling effect cannot be taken into account in the potential model, where a single partial wave is included.

V. CONCLUSIONS

The main goal of the present work is twofold: to update the microscopic calculation of DB94 and to evaluate the theoretical uncertainties associated with the extrapolation procedure. As already observed in other systems, increasing the number of generator coordinates in the ^{7}Be nucleus does not significantly affect the $^7\mathrm{Be}+p$ wave functions. In DB94, a single, but optimized value was used, and this seems to be a good approximation. On the other side, S_{17} is more sensitive to the *NN* interaction. The use of the MN force reduces the discrepancy between theory and experiment concerning the normalization. The difference in the energy dependence is, at most, 5% near 1.5 MeV.

We have analyzed different sources of theoretical uncertainties. Below 1 MeV the uncertainty is essentially due to the scattering length, which is currently known with an error bar of about 50% [27]. With direct capture data, which go down to energies as low as 150 keV, better knowledge of the scattering length seems to be sufficient to reduce uncertain-

TABLE V. $^7\mathrm{Be}(\mathrm{p},\gamma)^8\mathrm{B}$ S factor (in eV b). The decomposition refers to the MN force.

E (MeV)	MN	V2	$J=1^-$	$J=2^-$	$J=3^-$	$S=1,L=0$	$S=1,L=2$	$S=2,L=0$	$S=2,L=2$
0	24.69	29.45	3.99	19.77	0.93	3.87	0.26	19.29	1.27
0.02	24.01	28.63	3.85	19.09	1.07	3.72	0.30	18.53	1.47
0.05	23.24	27.68	3.69	18.26	1.28	3.53	0.35	17.59	1.76
0.1	22.57	26.85	3.53	17.43	1.61	3.32	0.44	16.59	2.21
0.15	22.34	26.55	3.43	16.98	1.93	3.19	0.53	15.97	2.65
0.2	22.37	26.56	3.39	16.74	2.24	3.11	0.62	15.57	3.07
0.25	22.57	26.75	3.36	16.65	2.55	3.04	0.70	15.32	3.50
0.3	22.87	27.06	3.36	16.64	2.87	3.00	0.79	15.15	3.93
0.35	23.23	27.45	3.36	16.69	3.18	2.97	0.88	15.04	4.35
0.4	23.64	27.88	3.37	16.77	3.49	2.94	0.96	14.96	4.78
0.45	24.07	28.34	3.38	16.87	3.81	2.91	1.05	14.90	5.21
0.5	24.49	28.81	3.39	16.97	4.13	2.88	1.14	14.84	5.64
0.6	25.42	29.72	3.48	17.17	4.78	2.89	1.31	14.70	6.52
0.7	26.24	30.57	3.50	17.30	5.44	2.83	1.50	14.50	7.41
0.8	27.00	31.35	3.52	17.37	6.11	2.78	1.68	14.22	8.32
0.9	27.67	32.06	3.54	17.35	6.79	2.72	1.87	13.83	9.25
1	28.28	32.70	3.54	17.25	7.48	2.65	2.07	13.36	10.20
1.1	28.82	33.30	3.54	17.09	8.19	2.58	2.27	12.79	11.19
1.2	29.32	33.87	3.54	16.87	8.91	2.50	2.47	12.14	12.20
1.3	29.79	34.45	3.54	16.61	9.64	2.42	2.69	11.43	13.25
1.4	30.26	35.06	3.55	16.33	10.38	2.34	2.91	10.67	14.33
1.5	30.74	35.71	3.56	16.05	11.13	2.26	3.15	9.88	15.46
1.6	31.25	36.42	3.58	15.78	11.89	2.18	3.39	9.07	16.62
1.7	31.82	37.21	3.61	15.54	12.67	2.10	3.64	8.25	17.83
1.8	32.44	38.11	3.66	15.33	13.45	2.02	3.90	7.44	19.09
1.9	33.15	39.11	3.72	15.18	14.25	1.95	4.17	6.65	20.39
2	33.94	40.24	3.79	15.10	15.05	1.87	4.45	5.89	21.73
2.1	34.81	41.48	3.87	15.08	15.86	1.80	4.74	5.17	23.11
2.2	35.79	42.86	3.97	15.14	16.68	1.73	5.03	4.51	24.52
2.3	36.86	44.37	4.09	15.28	17.50	1.66	5.34	3.90	25.97
2.4	38.06	46.05	4.21	15.51	18.34	1.59	5.65	3.35	27.47
2.5	39.39	47.89	4.35	15.83	19.21	1.52	5.98	2.86	29.03
2.6	40.85	49.90	4.50	16.25	20.09	1.44	6.32	2.45	30.63
2.7	42.41	52.03	4.66	16.76	20.99	1.37	6.66	2.11	32.26
2.8	44.04	54.25	4.83	17.35	21.87	1.30	7.00	1.86	33.88
2.9	45.72	56.52	5.00	18.00	22.72	1.23	7.34	1.69	35.46
3	47.43	58.81	5.18	18.72	23.54	1.17	7.66	1.60	37.00

ties due to the extrapolation below 1%. Near 1.5 MeV, which is more typical of breakup data, the *NN* interaction plays a dominant role. This sensitivity seems to be difficult to avoid.

We have performed a comparison with the potential model [17] which provides a different energy dependence. This is due to some limitations of the potential model: ^{7}Be deformation and channel coupling are absent. As long as spectroscopy only is concerned, these missing effects are simulated by an appropriate choice of spectroscopic factors. This might be possible with continuum states, but would probably require effective nucleus-nucleus potentials.

The present GCM model has been applied to the ^{8}B and ^{8}Li spectroscopy, with the goal of testing the wave functions. We basically confirm the results of DB94, but we provide additional information on ANC's and spectroscopic factors. The ANC's of ^{8}B and ^{8}Li are found very similar to each other, as expected from experiment [41]. In general, the spectroscopic factors are in good agreement with experiment. Our calculation predicts that the $5+3$ component in the ground state of ^{8}Li and ^{8}B is important and amounts to about 30%. A similar effect has been observed in ^{6}He where the dominant configuration is $\alpha+n+n$, but where the $t+t$ channel, although much higher in the ^{6}He spectrum, plays a role [64]. An experimental confirmation of this unexpectedly large component in ^{8}Li or ^{8}B would be welcome.

ACKNOWLEDGMENTS

I am grateful to B. Davids, A. Junghans, and K. Sümmerer for providing me with their experimental data and to C. Angulo for helpful comments about the manuscript. This text presents research results of the Belgian program P5/07 on interuniversity attraction poles initiated by the Belgian-state Federal Services for Scientific, Technical and Cultural Affairs.

APPENDIX

In this appendix we provide S_{17} in a numerical format. For the MN force, we use two decompositions: according to the total angular momentum J and according to the (S,L) partial waves (see Table V).

[1] SNO Collaboration, S. N. Ahmed *et al.*, Phys. Rev. Lett. **92**, 181301 (2004).
[2] S. Watanabe and H. Shibahashi, Publ. Astron. Soc. Jpn. **53**, 565 (2001).
[3] S. Couvidat, S. Turck-Chièze, and A. G. Kosovichev, Astrophys. J. **599**, 1434 (2003).
[4] J. N. Bahcall and M. H. Pinsonneault, Phys. Rev. Lett. **92**, 121301 (2004).
[5] J. N. Bahcall, *Neutrino Astrophysics* (Cambridge University Press, Cambridge, England, 1989).
[6] A. R. Junghans *et al.*, Phys. Rev. C **68**, 065803 (2003).
[7] F. Hammache *et al.*, Phys. Rev. Lett. **80**, 928 (1998); F. Hammache *et al.*, *ibid.* **86**, 3985 (2001).
[8] M. Hass, C. Broude, V. Fedoseev, G. Goldring, G. Huber, J. Lettry, V. Mishin, H. J. Ravn, V. Sebastian, L. Weissman, and the ISOLDE Collaboration, Phys. Lett. B **462**, 237 (1999).
[9] F. Strieder *et al.*, Nucl. Phys. **A696**, 219 (2001).
[10] L. T. Baby, C. Bordeanu, G. Goldring, M. Hass, L. Weissman, V. N. Fedoseyev, U. Koster, Y. Nir-el, G. Haquin, H. W. Gaggeler, R. Weinreich, and the ISOLDE Collaboration, Phys. Rev. C **67**, 065805 (2003); **69**, 019902(E) (2004).
[11] B. Davids *et al.*, Phys. Rev. Lett. **86**, 2750 (2001).
[12] F. Schumann *et al.*, Phys. Rev. Lett. **90**, 232501 (2003).
[13] P. Descouvemont, *Theoretical Models for Nuclear Astrophysics* (Nova Science, New York, 2003).
[14] F. C. Barker, Nucl. Phys. **A588**, 693 (1995).
[15] R. G. H. Robertson, Phys. Rev. C **7**, 543 (1973).
[16] S. Typel, H. H. Wolter, and G. Baur, Nucl. Phys. **A613**, 147 (1997).
[17] B. Davids and S. Typel, Phys. Rev. C **68**, 045802 (2003).
[18] P. Descouvemont and D. Baye, Nucl. Phys. **A567**, 341 (1994).
[19] A. Csótó, K. Langanke, S. E. Koonin, and T. D. Shoppa, Phys. Rev. C **52**, 1130 (1995).
[20] A. Csótó and K. Langanke, Nucl. Phys. **A636**, 240 (1998).
[21] L. Trache, A. Azhari, F. Carstoiu, H. L. Clark, C. A. Gagliardi, Y.-W. Lui, A. M. Mukhamedzhanov, X. Tang, N. Timofeyuk, and R. E. Tribble, Phys. Rev. C **67**, 062801 (2003).
[22] R. F. Christy and I. Duck, Nucl. Phys. **24**, 89 (1961).
[23] A. B. Volkov, Nucl. Phys. **74**, 33 (1965).
[24] D. Baye and N. K. Timofeyuk, Phys. Lett. B **293**, 13 (1992).
[25] P. Descouvemont and M. Dufour, Nucl. Phys. **A738**, 150 (2004).
[26] D. R. Thompson, M. LeMere, and Y. C. Tang, Nucl. Phys. **A286**, 53 (1977).
[27] C. Angulo *et al.*, Nucl. Phys. **A716**, 211 (2003).
[28] P. Descouvemont and D. Baye, Phys. Rev. C **36**, 54 (1987).
[29] K. Langanke, Adv. Nucl. Phys. **21**, 85 (1994).
[30] K. Wildermuth and Y. C. Tang, in *A Unified Theory of the Nucleus*, edited by K. Wildermuth and P. Kramer (Vieweg, Braunschweig, 1977).
[31] Y. C. Tang, *Topics in Nuclear Physics II*, Vol. 145 of Lecture Notes in Physics (Springer, Berlin, 1981), p. 572.
[32] D. Baye, P.-H. Heenen, and M. Libert-Heinemann, Nucl. Phys. **A291**, 230 (1977).
[33] D. Baye and N. Pecher, Bull. Cl. Sci., Acad. R. Belg. **67**, 835 (1981).
[34] R. J. Smith, J. J. Kolata, K. Lamkin, A. Morsad, F. D. Becchetti, J. A. Brown, W. Z. Liu, J. W. Jänecke, D. A. Roberts, and R. E. Warner, Phys. Rev. C **43**, 2346 (1991).
[35] J. A. Brown, F. D. Becchetti, J. W. Jänecke, K. Ashktorab, D. A. Roberts, J. J. Kolata, R. J. Smith, K. Lamkin, and R. E. Warner, Phys. Rev. Lett. **66**, 2452 (1991).
[36] P. Descouvemont and D. Baye, Phys. Lett. B **292**, 235 (1992).
[37] F. Ajzenberg-Selove, Nucl. Phys. **A490**, 1 (1988).
[38] T. Minamisono, J. W. Hugg, D. G. Mavis, T. K. Saylor, S. M. Lazarus, H. F. Glavish, and S. S. Hanna, Phys. Rev. Lett. **34**,

1465 (1975).
[39] A. M. Mukhamedzhanov *et al.*, Phys. Rev. C **56**, 1302 (1997).
[40] N. K. Timofeyuk, D. Baye, and P. Descouvemont, Nucl. Phys. **A620**, 29 (1997).
[41] N. K. Timofeyuk, R. C. Johnson, and A. M. Mukhamedzhanov, Phys. Rev. Lett. **91**, 232501 (2003).
[42] A. Azhari, V. Burjan, F. Carstoiu, C. A. Gagliardi, V. Kroha, A. M. Mukhamedzhanov, F. M. Nunes, X. Tang, L. Trache, and R. E. Tribble, Phys. Rev. C **63**, 055803 (2001).
[43] B. K. Jennings, Phys. Rev. C **62**, 027602 (2000).
[44] D. Baye, Phys. Rev. C **62**, 065803 (2000).
[45] T. Fliessbach and H. Walliser, Nucl. Phys. **A377**, 84 (1982).
[46] S. Saito, S. Okai, R. Tamagaki, and M. Yasuno, Prog. Theor. Phys. **50**, 1561 (1973).
[47] K. Varga and R. G. Lovas, Phys. Rev. C **37**, 2906 (1988).
[48] D. Cortina-Gil *et al.*, Phys. Lett. B **529**, 36 (2002).
[49] R. D. Macfarlane and J. B. French, Rev. Mod. Phys. **32**, 567 (1960).
[50] J. P. Schiffer, G. C. Morrison, R. H. Siemssen, and B. Zeidman, Phys. Rev. **164**, 1274 (1967).
[51] L. Koester, K. Knopf, and W. Waschkowski, Z. Phys. A **312**, 81 (1983).
[52] M. Wiescher, R. Steininger, and F. Käppeler, Astrophys. J. **344**, 464 (1989).
[53] M. Heil, F. Käppeler, M. Wiescher, and A. Mengoni, Astrophys. J. **507**, 997 (1998).
[54] J. C. Blackmon, A. E. Champagne, J. K. Dickens, J. A. Harvey, M. A. Hofstee, S. Kopecky, D. C. Larson, D. C. Powell, S. Raman, and M. S. Smith, Phys. Rev. C **54**, 383 (1996).
[55] W. L. Imhof, R. G. Johnson, F. J. Vaughn, and M. Walt, Phys. Rev. **114**, 1037 (1959).
[56] R. H. Cyburt, B. Davids, and B. K. Jennings, Phys. Rev. C **70**, 045801 (2004).
[57] P. D. Parker, Phys. Rev. **150**, 851 (1966).
[58] R. W. Kavanagh, T. A. Tombrello, J. M. Mosher, and D. R. Goosman, Bull. Am. Phys. Soc. **14**, 1209 (1969).
[59] F. J. Vaughn, R. A. Chalmers, D. Kohler, and L. F. Chase, Phys. Rev. C **2**, 1657 (1970).
[60] T. Kikuchi *et al.*, Eur. Phys. J. A **3**, 213 (1998).
[61] N. Iwasa *et al.*, Phys. Rev. Lett. **83**, 2910 (1999).
[62] K. Sümmerer (private communication).
[63] F. C. Barker and A. M. Mukhamedzhanov, Nucl. Phys. **A673**, 526 (2000).
[64] L. Giot *et al.*, Nucl. Phys. **A738**, 426 (2004).